# Vitrification of Nuclear Wastes

4

# Atomistic Design of $TiO_2$ Doped Sodium Borosilicate Glass

**Pooja Sahu[1,2], Sk. Musharaf Ali*[1,2], K. T. Shenoy[1], A. Arvind[3], D. Banerjee[3], Sanjay Kumar[3] and S. Manohar[3]**

[1]*Chemical Engineering Division, Bhabha Atomic Research Centre, Mumbai – 400085, INDIA*
[2]*Homi Bhabha National Institute, Anushaktinagar, Mumbai – 400094, INDIA*
[3]*Nuclear Recycle Group, Bhabha Atomic Research Centre, Mumbai – 400085, INDIA*

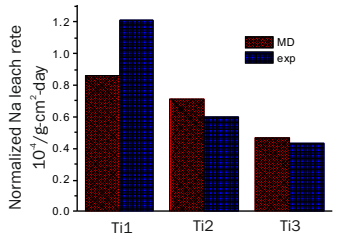


*Effect of $TiO_2$ concentration on Na leach rate.*

ABSTRACT

Selection of a suitable doping oxide for incorporation in sodium borosilicate glass for radioactive waste immobilization is one of the key challenges in nuclear waste management. Atomic simulations provide a route for initial screening and thus lessen the time and number of trial experiments. In that perspective, robust molecular dynamics (MD) simulations were carried out to identify the role of $TiO_2$ in augmenting mechanical, chemical and thermal strength of NBS glass. Computed results were well matched with the experimental findings. The present computational and experimental findings might be useful in the future design of NBS glass for nuclear waste immobilization.

KEYWORDS: *Sodium borosilicate glass, Nuclear waste management, Molecular dynamics, Nuclear waste immobilization*

## Introduction

The application of borosilicate glasses in radioactive waste immobilization [1, 2] arises due to a combination of useful material properties including high chemical durability, resistance to crystallization/devitrification and the ability to accommodate a wide diversity of cations within its structure. Basic understanding about the macroscopic properties of the glasses is pursued through microscopic structure at the atomic and molecular level. Considering the numerous applicability, and improved performance of titanium (Ti) added glass and glass ceramics, significant research has been conducted in this direction [3, 4, 5, 6]. Owing to high field strength and polarization ability of titanium ions, $TiO_2$ doped optical glasses have been profoundly used for optical applications [4, 6]. Besides, $TiO_2$ is used as a fascinating component in glass jewels and crystal wares. In addition, a decrease in viscosity of glass melts and improved mechanical strength of vitrified glasses can be achieved by increasing the $TiO_2$ content of the waste form [7]. The lack of understanding about the microscopic structure of these glasses and the local environment around Ti ions is the centre of the problem while dealing with optimization of Ti doped glasses for numerous applications.

Owing to their low solubility, it is difficult to experimentally synthesize the Ti doped silicate glasses. It has been observed that the presence of modifier ions offers the ease possibility of introducing Ti and other rare earth metal ions in the glass network. In absence of modifiers, doping of Ti and other rare earth metal ions can't be reach to high values as they tend to form cluster in these glasses [8, 9].

In spite of technical challenges, the peculiar behaviour of $TiO_2$ bearing glasses is still not fully understood. A large discrepancy has been noticed about the preferential occurrence of $TiO_4$, $TiO_5$ and $TiO_6$ structural forms in Ti doped glasses [5, 10, 11]. Therefore, a systematic investigation is needed to draw an appropriate conclusion. Very little to nothing has been reported about the effects of $TiO_2$ on the mechanical and other properties of ternary sodium borosilicate glasses [4, 12, 13].

The present article is devoted to understand the effects associated with the doping of titanium ions in sodium borosilicate glasses using molecular dynamics (MD) simulations. Though the experimental techniques continue to be the major source for finding the structural information and properties of materials, the recent advancement in MD like computational techniques may provide more valuable facts in many circumstances, especially when it is difficult to perform appropriate experiments. MD is extensively used to provide the microscopic insights, which might explain the experimentally observed phenomena.

## Computational Protocols

The glass simulations were conducted with LAMMPS package [14]. The interaction between atoms was simulated using the combination of Buckingham potential (for short-range interactions) and Coulomb potential (for long-range interactions), together known as Van Beest, Kramer, Van Santen (BKS) potential model [15].

$$U_{vdw} = \sum_{i=1}^{N}\sum_{j>i}^{N} A_{ij} e^{-r_{ij}/\rho_{ij}} - \frac{C_{ij}}{r_{ij}^6} \quad (1)$$

$$U_{coul} = \frac{q_i q_j}{4\pi\varepsilon r_{ij}} \quad (2)$$

The parameters $\rho_{ij}$, $A_{ij}$ and $C_{ij}$ control the narrowness of potential model. The separation between the $i^{th}$ and $j^{th}$ atom, having partial charge $q_i$ and $q_j$ respectively is represented by $r_{ij}$ and $\varepsilon$ is the permittivity. The forcefield parameters of simulated glasses can be found in our previous papers[16, 17].

Particle-Particle-Particle Mesh (PPPM) method[18] was employed to account for the long-range interactions. The

*Author for Correspondence: Sk. Musharaf Ali
E-mail: musharaf@barc.gov.in

partial charge on the atoms were taken to be composition dependent [19]. All systems were initially heated at 5000 K using the canonical (NVT) ensemble for 10 ns in order to remove the memory effects. This was followed by NVT quenching at a rate of 0.4 K/ps. The systems were furthermore equilibrated for 20 ns dynamics using the isothermal–isobaric ensemble (NPT)[20] at 300 K and P = 1 atm. Further, the production runs were performed for 30 ns, and the generated data was utilized for the analysis of structural and dynamical properties of simulated glass, with methods as discussed in our earlier articles. [16, 17].

## Results and Discussion

Titanium dioxide does not form a glass alone, but it can be incorporated in significant amounts into other glass-forming oxide systems. The addition of $TiO_2$ to glasses contributes to improve glass-forming ability, chemical durability and stabilization of the glass structure. In general, vitrified sodium borosilicate glass for nuclear applications contain $TiO_2$ concentration less than 1% weight [21]. However, for optical and other applications, the role of $TiO_2$ with concentration 0-30% in ternary and quaternary borosilicate glasses [11, 22-25] and 0-50% in binary silicate glasses[5, 26, 11] have been studied in the light of experiments and MD simulations. In the present study, the sodium borosilicate (NBS) doped with $TiO_2$ molar composition varied from 2% to 20% were considered. For all the simulated glasses, the numbers of $SiO_2$, $B_2O_3$ and $Na_2O$ molecules were kept constant as 680, 340 and 238 respectively, whereas the number of $TiO_2$ was varied to be 25, 63, 126, 189, 252, 314 and 378. The percentage contribution of $TiO_2$ was varied from 1.95%, 4.77%, 9.10%, 13.06%, 16.69% and 19.97%, denoted as Ti1, Ti2, Ti3, Ti4, Ti5, and Ti6 respectively. The corresponding simulated snapshots are shown in Fig. 1.

The computed density was seen to increase with increasing $TiO_2$ concentration in the glass matrix (Fig.2). The increase in density with increasing Ti concentration was supposed to be related with the higher molecular weight (79.87 g $mol^{-1}$) of $TiO_2$ than the other components ($SiO_2$ = 60.08 g $mol^{-1}$, $B_2O_3$ = 69.62 g $mol^{-1}$, $Na_2O$ = 61.98 g $mol^{-1}$).

In addition to density, the volume of glass was also increased while increasing $TiO_2$, as network structure was found to expand with increasing $TiO_2$ due to formation of more [$BO_3$] units. However, the density was dominated by increase in mass of the matrix rather than the volume. The observed pattern for increasing density with increasing $TiO_2$ concentration agrees with the studies of Bernard et al. [5]. Additionally, the NBO were decreased from 18.5% to 12.9%, while increasing $TiO_2$ concentration from 2% to 20% in Ti-NBS glasses.

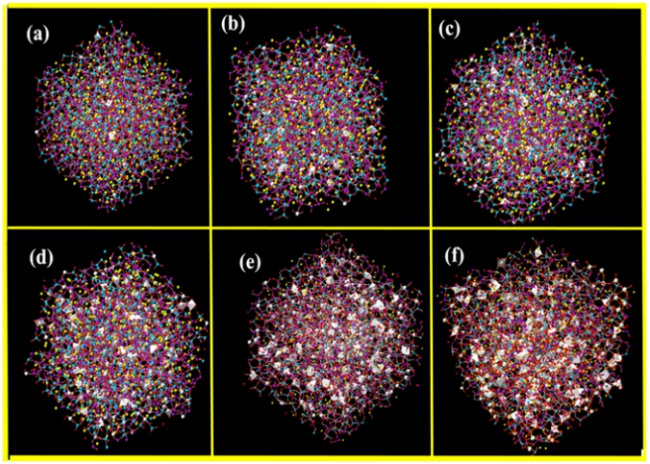


*Fig.1: Snapshot of Ti-NBS glasses with (a) 1.95%, (b) 4.77%, (c) 9.10%, (d) 13.06%, (e) 16.69% and (f) 19.97%, $TiO_2$ concentration captured at 50ns [Si: cyan, B: purple, Na: yellow, O:red, Ti: white polyhedral].*

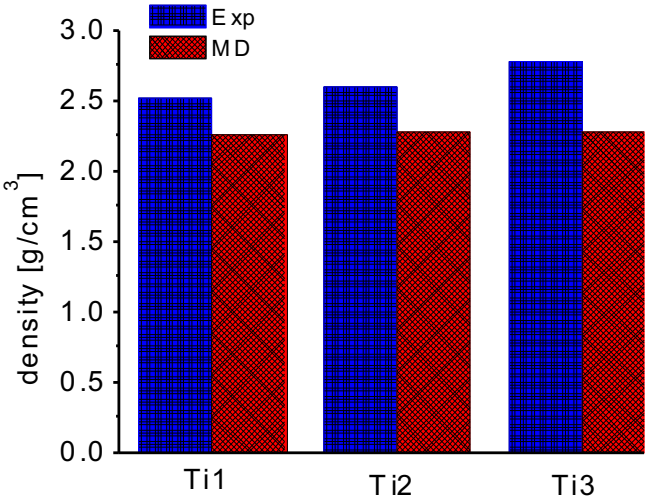


*Fig.2: $TiO_2$ concentration effect on density of NBS glass.*

Even at highest $TiO_2$ concentration of 20% in Ti-NBS glasses, the $TiO_2$ seems to be distributed throughout the glass network as shown in Fig.3(I) and Fig.3(ii). The presence of Ti-O-Ti linking along with Ti-O-Si and Ti-O-B was also observed in the simulated glasses. The snapshot of Ti-O-Ti chain is shown in Fig.3(iii) and Fig.3(vi) respectively. Interestingly, titanium ions in the glass network were observed in $TiO_6$ and $TiO_5$ structural forms. The octahedral structure of $TiO_6$ and square pyramid structure of $TiO_5$ is shown in Fig.3(iv) and Fig.3(v) respectively. Fig.3(vii) to Fig.3(x) indicate different structural forms of Ti-Ti connection, such as Ti-Ti connected with two shared oxygen atoms, and three shared oxygen atoms. To be noted, no $Ti^{4+}$ was found in $TiO_4$ tetrahedral form in the Ti-NBS glasses. This shows that multi-coordinated Ti ions, do not change from octahedral to tetrahedral coordination by isomorphically replacing $SiO_4$ tetrahedrals. The absence of $TiO_4$ structural form has also been supported by the studies of Kukharenko et al. [22] as well as Osipov et al.[10].

## Network Strength

The network connection was demonstrated by estimating the probable distribution for connecting network

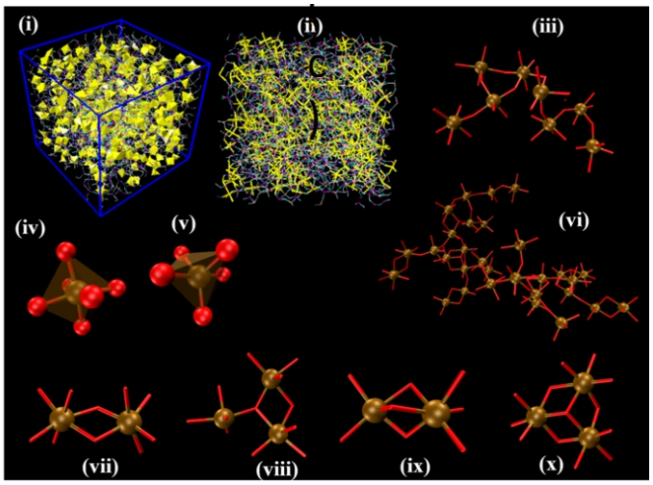


*Fig.3: (i, ii) Snapshot representing the distribution of $TiO_n$ polyhedral in the glass network, (iii, vi) images representing Ti-Ti chain network in the glass; (iv, v) $TiO_6$ and $TiO_5$ structural forms of Ti; (vii-x) Ti-Ti connectivity with two and three shared oxygen atoms.*

formers with methodologies as used in our previous article[16].

The results in Fig.4 show the order of preference as Si-O-B4 > Si-O-B3 > Si-O-Si > B3-O-B4 > Si-O-Ti > B3-O-B3 > B4-O-B4 > B3-O-Ti > B4-O-Ti > Ti-O-Ti for Ti1; Si-O-B4 > Si-O-B3 > Si-O-Si > Si-O-Ti > B3-O-B4 > B3-O-B3 > B3-O-Ti > B4-O-B4 > B4-O-Ti > Ti-O-Ti for Ti2; Si-O-B3 > Si-O-B4 > Si-O-Ti > Si-O-Si > B3-O-B4 > B3-O-Ti > B3-O-B3 > B4-O-Ti > B4-O-B4 > Ti-O-Ti for Ti3; Si-O-B3 > Si-O-Ti > Si-O-B4 > Si-O-Si > B3-O-Ti > B3-O-B3 > B3-O-B4 > B4-O-Ti > Ti-O-Ti > B4-O-B4 for Ti4; Si-O-Ti > Si-O-B3 > B3-O-Ti > Si-O-Si > Si-O-B4 > B3-O-B3 > B3-O-B4 > Ti-O-Ti > B4-O-Ti > B4-O-B4 for Ti5; and Si-O-Ti > Si-O-B3 > B3-O-Ti > Si-O-Si > Si-O-B4 > B3-O-B3 > Ti-O-Ti > B3-O-B4 >B4-O-Ti > B4-O-B4 for Ti6 (B3: $BO_3$, and B4: $BO_4$).

Snapshot for connectivity of polyhedrals is shown in Fig.5. Results show that with the sufficient presence of B4 fraction (x>30%), the Si-O-B connections are favored over Si-O-Si connections. For Ti1 and Ti2, where B4 fraction is x>45%, the Si-O-B4 > Si-O-B3 > Si-O-Si order was followed, however, with B4 fraction 30% - 40%, the order was changed to Si-O-B3 > Si-O-B4 > Si-O-Si and then for B4 fraction below than 30%, it was Si-O-B3 > Si-O-Si > Si-O-B4. Our results showed abundant presence of B4-O-B4 connections.

Though all three B3–O–B4, B3–O–B3, and B4–O–B4 links were present, the probability of connecting B4-O-B4 was always minimum among the three. However, for higher B4 fraction (i.e., Ti1, Ti2 and Ti3), the intermixing of B3 and B4 i.e., B3-O-B4 connections were found to be preferred over either of B3-O-B3 or B4-O-B4 connections. On the other hand, for lower B4 fraction (system Ti4, Ti5 and Ti6), the order was followed as B3–O–B3 > B3–O–B4 > B4–O–B4. Our results are in agreement with the studies of Yu et al.[27] who showed that the presence of $B_p$-O-$B_q$ motifs (p and/or q is equal to 3 and/or 4) is primarily controlled by the fraction of B4 and NBO content.

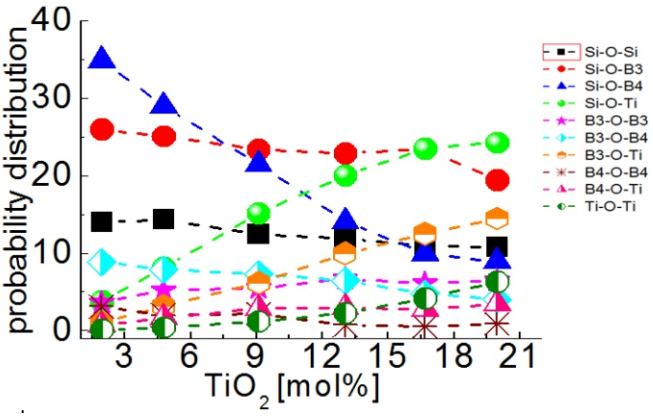


*Fig.4: Probability distribution profile for preferential connection of various (X-O-X′; where X and/or X′=$SiO_2$, $BO_3$, $BO_4$, and $TiO_n$) structural units in simulated Ti-NBS glass compositions.*

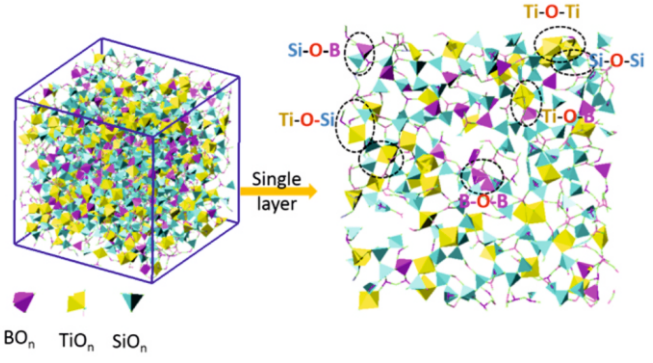


*Fig.5: Image representing the connectivity of different polyhedrals in Ti-NBS glass.*

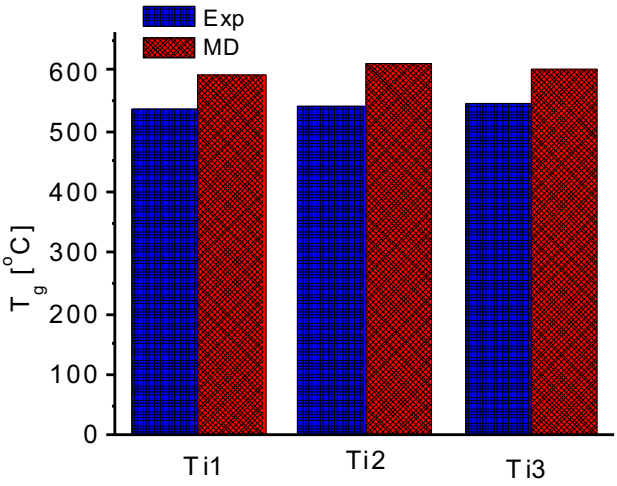


*Fig.6: Effect of $TiO_2$ concentration on the glass transition temperature of Ti-NBS glass.*

## Thermal Strength

The fabrication easiness was analyzed in terms of glass transition temperature ($T_g$). The estimated glass transition temperature of simulated glasses is shown in Fig.6. The results show increasing Tg with $TiO_2$ addition in base NBS glass matrix. The same was also expected from the increasing BOs with Ti addition in Ti-NBS glasses. Though with $TiO_2$ addition, $BO_3$ fraction is increased, which is known to reduce the melting temperature, however, the increasing Tg with $TiO_2$ addition in Ti-NBS glasses seems to be linked with the increased strength of glass skeleton with $TiO_2$ doping. Hereby, results show that $TiO_2$ addition would increase the melting temperature during glass fabrication process.

## Chemical Strength

In order to understand the chemical durability which measures the strength of the glass in contact with water, the interaction of NBS and Ti-NBS glass was studied. The glass-water system was modelled by keeping the amorphous structure of glass in adjacent to a box containing 2000 number of water molecules(TIP4P/2005 water model). The interaction between glass atoms and water molecules was estimated using Lennard-Jones potential model. The final snapshot in Fig.7 shows that some of sodium ions are diffused from bulk glass region to the interface, while few of them were migrated to the bulk aqueous phase. Mass density profiles of atoms O, Na and $O_w$ for NBS and Ti-NBS systems are shown in Fig.8. Results show the accumulation of Na ions near the water side of interface, whereas, presence of sodium depleted zone at the glass side of interface.

Also, compared to bulk region, the density of water molecules was observed to be higher near the interface where accumulation of Na ions was noticed. This shows the structuring of water molecules and accumulated sodium ions at the glass-water interface. Also, the glass-water interface seems to be sharper for Ti-NBS than the NBS glass, may be due to reduced accumulation of sodium ions at the interface for Ti-NBS glass than the NBS glass. Apart from this, one can also observe the diffusion and accumulation of water molecules in sodium depleted zone of glass. Few water molecules were even migrated to bulk glass phase as shown by density profiles. Interestingly, water molecules were found to diffuse into glass network in its intact form. Hereby, it can be stated that water

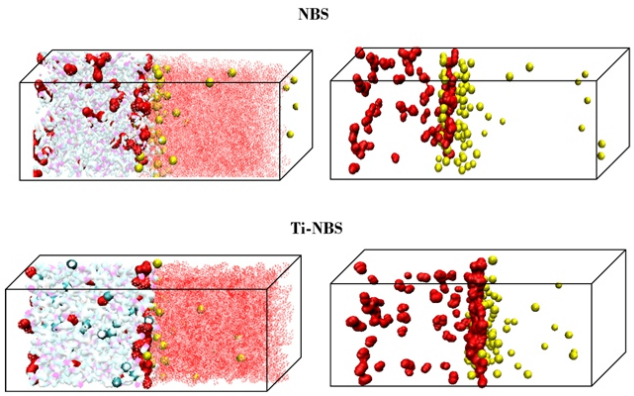


*Fig.7: Snapshot representing Na leaching to interface and bulk aqueous phase, and water diffusion to glass regime for NBS and Ti-NBS glass from MD simulations [glass matrix - Si: cyan, B: magenta, Ti: cyan, Na: yellow balls; aqueous water shown by solvent style with red color; water extracted to glass side of interface and bulk glass regime shown by red quick surface style].*

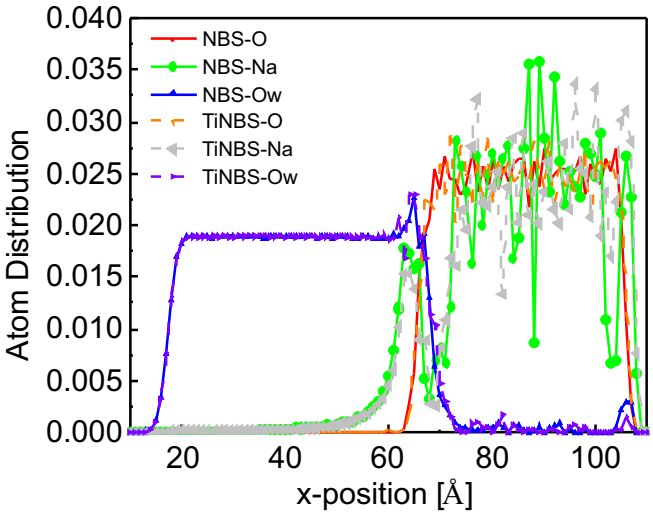


*Fig.8: Atom distribution profile for $O_{water}$, $O_{glass}$ and Na ions for NBS and Ti-NBS glasses.*

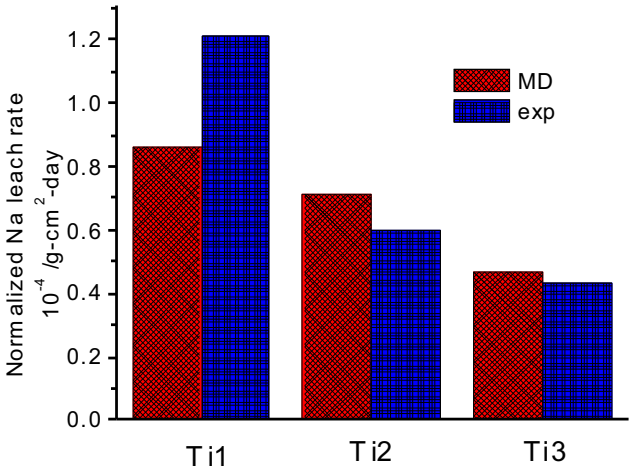


*Fig.9: Effect of $TiO_2$ concentration on Na leach rate.*

molecules can enter in the glass network without being chemically reacted with the glass network. Furthermore, the dividing boundaries of mass density profiles for atoms O and $O_w$ were used to evaluate the interface position. The interfacial region was decided to be of 5Å thickness across the intersection point and region beyond that was considered as bulk phase of water and glass respectively. Interestingly, the adsorption of water molecules was found to affect the glass structure considerably for surface region and marginally for bulk region. The density of glass atoms was reduced by half at glass surface (0.57g/cm$^3$) compared to bulk region (1.36 g/cm$^3$).

The number of accumulated Na ions at the interface as well as the number of Na ions migrated to bulk aqueous phase was found to be considerably reduced for Ti-NBS glass compared to NBS glass (data shown in Fig.9). This leads to a significant decrease in total number of Na ions leached from the glass to aqueous solution while Ti doping of NBS glass. On contrary to sodium ions, the number of water molecules migrated from bulk aqueous phase to interface as well as the bulk glass region was found to be increasing with Ti doping of NBS glass, which might be linked with the higher concentration of alkali ions in Ti-NBS than NBS, remained after keeping them in contact with aqueous solution.

The computed results show that leaching of Na ions can be controlled by $TiO_2$ doping of NBS glasses. In particular, for Ti-NBS glasses, the $TiO_n$ connected $Na^+$ ions are strongly attached to glass network and are less likely to move compared to free $Na^+$ ions in bare NBS glass matrix. As a result, Ti bearing glasses will be less prone to leaching when exposed to aqueous environment compared to Ti free NBS glasses. In other words, the chemical durability of sodium borosilicate glasses is supposed to increase with doping of $TiO_2$ [28].

## Summary and Conclusion

The present report demonstrates that BKS potential model with the selected forcefield parameters can be utilized to simulate the glasses with multi-component oxides. Admitting the advantageous effect of $TiO_2$ doping for optical and nuclear waste glasses, the present studies feature the behaviour of Ti-NBS glasses as function of $TiO_2$ concentration in the glass matrix. The modification in glass structure, mechanical integrity, thermal strength and chemical durability was probed using molecular dynamic simulations. Results report influence of Ti doping and concentration on important properties of borosilicate glasses. The results might be very helpful in prediction of effects associated with the dopant's nature and concentration. Hereby, the present results might have great academic as well technological significance for further guidance in the selection of dopant oxide for multi-component glass for nuclear waste immobilization.

## Acknowledgement

Computer division is acknowledged for providing 'ANUPAM' super computation facility. Pallavi Yevale and Annie Joseph of PSDD are thankfully acknowledged for glass experiments.

## References

[1] M. J. Plodinec, Glass Technol-part A, 2000, 41, 186-192.

[2] C. P. Kaushik, Procedia Mater. Sci., 2014, 7, 16-22.

[3] Janbandhu, S. Y.; Joshi, A.; Munishwar, S. R.; Gedam, R. S. Appl. Surf. Sci. 2019, 497, 143758.

[4] Azooz, M. A.; Aiad, T. H. M. A.; ElBatal, F. H.; ElTabii, G. Indian J. Pure Appl. Phys. 2008, 46, 880-888.

[5] Bernard, C.; Chaussedent, S.; Monteil, A.; Ferrari, M. Philos. Mag. B 2002, 82, 681-693.

[6] Karlsson, S.; Bäck, L. G.; Kidkhunthod, P.; Lundstedt, K.; Wondraczek, L. Opt. Mater. Express 2016, 6, 257129.

[7] Status and Trends in Spent Fuel and Radioactive Waste Management; IAEA Nuclear Energy: Series No. NW-T-1.14: 2018.

[8] Orignac, X.; Barbier, D.; Du, X. M.; Almeida, R. M.; McCarthy, O.; Yeatman, E. Opt. Mater. Express 1999, 12, 1-18.

[9] Orignac, X.; Vasconcelos, H. C.; Almeida, R. M. J. Non-Cryst. Solids 1997, 217, 155-161.

[10] Osipov, A. A.; Korinevskaya, G. G.; Osipova, L. M.; Muftakhov, V. A. Glass Phys. Chem. 2012, 38, 357-360.

[11] Marzouk, M. A.; ElBatal, F. H.; ElBatal, H. A. Opt. Mater. 2016, 57, 14-22.

[12] Morsi, M. M.; El-Shennawi, A. W. A. Phys. Chem. Glasses 1984, 25, 64-68.

[13] Strimple, J. H.; Giess, E. A. J. Am. Ceram. Soc. 1958, 41, 231-237.

[14] S. Plimpton, J. Comput. Phys., 1995, 117, 1-19.

[15] B. W. H. v. Beest, G. J. Kramer and R. A. v. Santen, Phys. Rev. Lett., 1990, 64, 1955-1958.

[16] P. Sahu, Sk. M. Ali, K. T. Shenoy, S. Mohan, A. Arvind, G. Sugilal and C. P. Kaushik, Phys. Chem. Chem. Phys., 2021, 23, 14898.

[17] P. Sahu, A. A. Pente, M. D. Singh, I. A. Chowdhri, K. Sharma, M. Goswami, S. M. Ali, K. T. Shenoy and S. Mohan, J. Phys. Chem. B, 2019, 123, 6290−6302.

[18] B. A. Luty and W. F. v. Gunsteren, J. Phys. Chem., 1996, 100, 2581–2587.

[19] L.-H. Kieu, J.-M. Delaye, L. Cormier and C. Stolz, J. Non-Crystal. Solids, 2011, 357, 3313–3321.

[20] M. P. Allen and D. J. Tildesley, Computer Simulation of Liquids, Clarendon Press, Oxford University, 2017.

[21] Manaktala, H. K. An Assessment of Borosilicate Glass as a Highlevel Waste Form Nuclear Regulatory Commission Contract NRC-02-88-005 (CNWRA 92-017), San Antonio, Texas, 1992.

[22] Kukharenko, S. A.; Shilo, A. E.; Itsenko, P. P.; Kutsai, A. N. T J. Superhard Mater. 2010, 32, 396-405.

[23] Ruengsri, S.; Kaewkhao, J.; Limsuwan, P. Procedia Eng. 2012, 32, 772-779.

[24] Limbach, R.; Karlsson, S.; Scannell, G.; Mathew, R.; Edén, M.; Wondraczek, L. J. Non-Cryst. Solids 2017, 471, 6-18.

[25] Farges, F.; Jr., G. E. B.; Navrotsky, A.; Gan, H.; Rehr, J. J. CGeochim Cosmochim Acta 1996, 60, 3039-3053.

[26] Scannell, G.; Huang, L.; Rouxel, T. J. Non-Cryst. Solids 2015, 429, 129–142.

[27] Yu, Y.; Stevensson, B.; Edén, M. J. Phys. Chem. Lett. 2018, 9, 6372–6376.

[28] P. Sahu, Sk. M. Ali, : Langmuir 2022, 38, 7639−7663.